Published in final edited form as:

Photochem Photobiol Sci. 2012 April ; 11(4): 653–660. doi:10.1039/c2pp05355a.

Photochemical Release of Methotrexate from Folate Receptor-Targeting PAMAM Dendrimer Nanoconjugate

Seok Ki Choi[a,b], **Thommey P. Thomas**[a,b], **Ming-Hsin Li**[a,c], **Ankur Desai**[a,b], **Alina Kotlyar**[a,b], and **James R. Baker Jr.**[a,b,c]

Seok Ki Choi: skchoi@umich.edu; James R. Baker: jbakerjr@umich.edu

[a]Michigan Nanotechnology Institute for Medicine and Biological Sciences, University of Michigan, Ann Arbor, MI 48109, USA

[b]Department of Internal Medicine, University of Michigan, Ann Arbor, MI 48109, USA

[c]Department of Biomedical Engineering, University of Michigan, Ann Arbor, MI 48109, USA. Fax: (+01) 734-615-0621; Tel: (+01) 734-615-0615

Abstract

Nanoparticle (NP)-based targeted drug delivery involves cell-specific targeting followed by a subsequent therapeutic action from the therapeutic carried by the NP system. NPs conjugated with methotrexate (MTX), a potent inhibitor of dihydrofolate reductase (DHFR) localized in cytosol, have been under investigation as a delivery system to target cancer cells to enhance the therapeutic index of methotrexate which is otherwise non-selectively cytotoxic. Despite improved therapeutic activity from MTX-conjugated NPs *in vitro* and *in vivo*, the therapeutic action of these conjugates following cellular entry is poorly understood; in particular it is unclear whether the therapeutic activity requires release of the MTX. This study investigates whether MTX must be released from a nanoparticle in order to achieve the therapeutic activity. We report herein light-controlled release of methotrexate from a dendrimer-based conjugate and provide evidence suggesting that MTX still attached to the nanoconjugate system is fully able to inhibit the activity of its enzyme target and the growth of cancer cells.

1. Introduction

One of primary objectives in targeted drug delivery is to enhance the therapeutic index of drugs by facilitating their selective drug uptake into target cells[1–7]. Nanoscale particles (NPs) functionalized with cancer cell targeting ligand(s) and drug(s) form nanoconjugates designed to undergo cellular internalization via specific receptors[2–3, 8–10]. This strategy has been successfully applied to the delivery of anti-cancer therapeutics such as methotrexate (MTX)[9–11], cisplatin[3], doxorubicin[12–13], and paclitaxel[1, 8]. The effectiveness of targeted nanoconjugate depends on several factors, including the shape and size of NP, drug density on the NP density, type of linker used to tether the drug molecule to the NP and, for certain types of drugs, the extent of drug release from the NP[4, 14–17]. This study seeks to determine

Correspondence to: Seok Ki Choi, skchoi@umich.edu; James R. Baker, Jr., jbakerjr@umich.edu.

whether MTX must be released from dendrimer NP in order to be fully active. We use a photochemical mechanism[13] to release the cytotoxic drug MTX from a dendrimer to inhibit the cytoplasm enzyme dihydrofolate reductase (DHFR)[18–19] (Figure 1). These studies provide evidence that MTX release from a dendrimer NP is not essential to achieve therapeutic activity.

Methotrexate, an anti-folate cytotoxic drug, functions by inhibiting dihydrofolate reductase[18, 20] (K_i = 0.0034 nM[21]), a cytosolic enzyme that catalyzes the reduction of dihydrofolate to tetrahydrofolate for the *de novo* biosynthesis of thymidine in DNA synthesis (see Figure 1b for a crystal structure of DHFR in complex with MTX[22]). Although MTX has efficient cytotoxic activity against cancer cells, it suffers from dose-limiting systemic toxicity that results in a narrow therapeutic index[23]. Because of this, MTX has been an attractive candidate for use in a variety of targeted therapeutic delivery systems. While some systems have relied on the encapsulation of MTX for drug delivery[24–25], MTX has been more commonly covalently attached to nanoscale carriers such as dendrimers[9, 11, 26–29], dextran[30], oligopeptide[31], albumin protein[32], and iron oxide nanoparticles[33] through either amide[28–33] or ester bonds[9, 11, 27]. These MTX nanoconjugates are cytotoxic *in vitro*, and some tested in *in vivo* tumor models displayed selective tumor targeting[27–29], prolonged systemic circulation[27–28, 30], and enhanced therapeutic index[27]. Despite the promising activity of these nanoconjugates, what happens to their drug payload following cellular entry is poorly understood. In particular, it is not clear to what extent MTX remains conjugated to the NP carrier system, and whether the release of this drug plays a significant role in the therapeutic activity of the nanoconjugate.

In a recent study,[11] we synthesized a nanoconjugate **1** (PAMAM-FA_4-MTX_5; Figure 1a), comprised of folic acid (FA), a high affinity ligand for the folic acid receptor (FAR; K_d = 0.4 nM)[34], and MTX, both attached to the surface of generation 5 polyamidoamine dendrimer (G5 PAMAM)[35]. This conjugate **1** was selectively internalized by KB cells through FAR-mediated endocytosis and was shown to inhibit cell growth[9]. In a study designed to determine the mechanism of drug action following cellular entry, we investigated the chemical stability of the MTX ester linkage of **1** under conditions that mimic the acidic environment of FAR-containing endosomes (pH ≈ 5 – 6.5)[36–37]. Our hypothesis was that acidic conditions would hydrolyze the ester linkage, thereby releasing the drug from the dendrimer. Interestingly, however, this conjugate was almost completely resistant to hydrolysis and failed to release MTX under either acidic or nonselective esterase-mediated *in vitro* conditions. In addition, the intact conjugate was shown to inhibit purified DHFR in a cell-free assay as effectively as free MTX[38]. The crystal structure (PDB 1u72)[22] of hDHFR in complex with a methotrexate molecule at its active site (Figure 1b) suggests that the tethered MTX molecule could inhibit the catalytic activity of DHFR if its linker is sufficiently long and flexible enough to allow the interaction at the enzyme-dendrimer interface.[39] These observations suggested that dendrimer-conjugated MTX could be active, but its exact role was not evaluated in the cytotoxic activity observed with drug conjugates. To further characterize the activity of an ester-linked MTX conjugate following cellular internalization, we used a strategy that provided consistent and precise control for the release of the MTX payload. In this communication, we report the design and synthesis

of a photo-releasable MTX-based nanoconjugate, demonstrate MTX release from the conjugate through a light-controlled mechanism[13] and evaluate its cytotoxic activity in KB cells following exposure to UV light.

2. Materials and methods

2.1 General synthetic methods

All solvents and reagents were purchased from commercial suppliers (Aldrich, Fluka, TCI), and used without further purification including folic acid dihydrate (Sigma; purity 98%), and methotrexate hydrate (TCI America; purity >98%). Reactions were run under nitrogen atmosphere unless noted otherwise. Progress of reactions was monitored by thin layer chromatography on Merck® TLC plates (250 μm thick), and spots were detected by UV illumination at 254 or 365 nm or by staining with phosphomolybdic acid reagent (20% w/v in ethanol) or ninhydrin solution (5% w/v in 3% acetic acid/ethanol). Reaction mixtures were worked up as described specifically in each reaction including flash column chromatography using silica gel (200–400 mesh). Characterization of reaction products was routinely carried out by ^{1}H NMR spectroscopy and mass spectrometry. For NMR (^{1}H, ^{13}C) measurement, samples were dissolved in deuterated solvent ($CDCl_3$, CD_3OD, D_2O, DMSO-d_6), and NMR spectra were acquired with a Varian nuclear magnetic resonance spectrometer at 400 MHz or 300 MHz for ^{1}H NMR spectra, and at 100 MHz for ^{13}C NMR spectra under standard observation conditions. Mass spectrometric identification of compounds was performed by electrospray ionization mass spectrometry (ESI-MS) with a Micromass AutoSpec Ultima spectrometer. Molecular masses of PAMAM G5 dendrimer and its conjugates were measured by matrix assisted laser desorption ionization-time of flight (MALDI-TOF) with a Waters TOfsPec-2E spectrometer. The MALDI spectra were acquired using a matrix solution of 2,5-dihydroxybenzoic acid (10 mg/ml in 50% aqueous acetonitrile) in a linear mode with a high mass detector. The spectrometer was mass calibrated with BSA in sinapinic acid, and data was acquired and processed using Mass Lynx 3.5 software. UV-vis absorption spectra were recorded on a Perkin Elmer Lamda 20 spectrophotometer. Size exclusion chromatography (SEC) was used to measure absolute molecular weights and polydispersity index (PDI) of PAMAM G5 dendrimer **6** by using an Alliance Waters 2690 separation module (Waters Corporation, Milford, MA) equipped with a Waters 2587 UV absorbance.

2.2 Synthesis of 3

The *ortho*-nitrobenzyl linker **3** was synthesized starting from 4-formyl-2-methyoxyphenol (vanillin) as pale yellow solid[13]. R_f (5% MeOH/$CHCl_3$) = 0.37. ^{1}H NMR (300 MHz, $CDCl_3$): δ = 7.73 (s, 1H), 7.33 (s, 1H), 4.98 (s, 2H), 4.55 (s, 2H), 4.00 (s, 3H), 3.45-3.40 (m, 2H), 3.29-3.25 (m, 2H), 1.40 (s, 9H) ppm; ^{13}C NMR (100MHz, $CDCl_3$): δ = 167.97, 154.52, 145.61, 139.52, 134.34, 112.18, 111.43, 69.21, 62.37, 56.38, 56.36, 40.36, 39.68, 28.24, 24.76 ppm; MS (ESI): *m/z* (relative intensity, %) = 422.2 (100) $[M+Na]^+$, 821.3 (20) $[2M+Na]^+$, 322.1 (13) $[M+Na\text{-}Boc]^+$; HRMS (ESI) calcd for $C_{17}H_{25}N_3O_8Na$ 422.1539, found 422.1533.

2.3 Synthesis of 4

To a cold solution of *ortho*-nitrobenzyl linker **3** (0.4 g, 1.0 mmol) and triethylamine (0.29 mL, 2.1 mmol) in $CHCl_3$ in ice bath was added methanesulfonyl chloride (0.082 mL, 1.1 mmol). After stirring for 1.5 h at 0°C, the solution was evaporated *in vacuo*, yielding pale beige solid (R_f = 0.5 in 10% MeOH/$CHCl_3$). It was dissolved in 4 mL of DMF, and used for the next step immediately. To a separate round bottomed flask containing DMF (25 mL) was added methotrexate hydrate (0.544 g, 1.1 mmol) and cesium carbonate (0.651 g, 2.0 mmol) grounded as fine powder. To this stirred mixture was added the DMF solution that contained the mesylate prepared previously, and sodium iodide (0.15 g, 1.0 mmol). The final mixture was stirred at rt for 27 h under nitrogen atmosphere in the dark, and evaporated *in vacuo* yielding pale yellow residue. It was dissolved in a small volume (~5 mL) of 5% MeOH/$CHCl_3$, and loaded onto a silica column. The reaction mixture was purified by eluting with 3 to 5% MeOH/$CHCl_3$ where the desired product was eluted with an R_f value of 0.53 (1% AcOH in 20% MeOH/$CHCl_3$). After evaporation of the desired fractions, solid was obtained, rinsed with MeCN and dried *in vacuo* yielding **4** as yellow solid (193 mg, 23%). ^{1}H NMR (400 MHz, DMSO-d_6): δ = 8.49 (s, 1H), 7.67 (m, 2H), 7.63 (s, 1H), 7.15 (s, 1H), 6.76 (m, 2H), 5.39 (s, 2H), 4.72 (s, 2H), 4.54 (s, 2H), 4.43 (br m, 1H), 3.83 (s, 3H), 3.15 (s, 3H), 3.10 (br, 2H), 2.94 (br, 2H), 2.24 (br, 2H), 1.80 (br, 2H), 1.29 (s, 9H) ppm; MS (ESI): *m/z* (relative intensity, %) = 836.4 (100) $[M+H]^+$, 736.4 (19) $[M+H\text{-Boc}]^+$, 1672.7 (2) $[2M+H]^+$; HRMS (ESI) calcd for $C_{37}H_{46}N_{11}O_{12}$ 836.3327, found 836.3325.

2.4 Synthesis of 5

To *N*-Boc protected methotrexate-linker **4** (31 mg, 37.1 μmol) was added a mixture of $CHCl_3$ (1.0 mL) and TFA (0.5 mL). The mixture was stirred at rt for 15 min, and evaporated to dryness *in vacuo* yielding pale yellow oil. The product was used immediately without further treatment for the coupling reaction with dendrimer **6**. ^{1}H NMR (300 MHz, DMSO-d_6): δ = 8.70 (d, 1H), 7.80 (m, 1H), 7.68-7.67 (m, 2H), 7.20 (m, 1H), 6.80 (t, 2H), 5.40-5.35 (m, 2H), 4.85 (d, 2H), 4.62 (br s, 3H), 3.94 (s, 3H), 3.36 (t, 2H), 3.24 (d, 3H), 2.87 (t, 2H), 2.68 (m, 2H), 2.20-2.10 (m, 2H) ppm; MS (ESI): *m/z* (relative intensity, %) = 736.2 (100) $[M+H]^+$, 1471.5 (3) $[2M+H]^+$, 308.1 (61); HRMS (ESI) calcd for $C_{32}H_{38}N_{11}O_{10}$ 736.2803, found 736.2824.

2.5 Synthesis of 7

Folic acid-ethylenediamine amide was prepared as described elsewhere[40]. To a stirred solution of folic acid dihydrate (1.0 g, 1.94 mmol) in DMF (120 mL) was added 1-ethyl-3-(3-dimethylaminopropyl)carbodiimide hydrochloride (2.0 g, 10.4 mmol). After stirring for 1 h in the dark, 1,2-diaminoethane (1.26 g, 21.0 mmol) was added to the solution prepared early, and the final solution was stirred at RT for 6 h. The mixture was concentrated to dryness *in vacuo* yielding yellow residue. It was dissolved in water (~10 mL), loaded onto a column (silica gel, 50 g), and flash chromatographed by eluting with 50% MeOH/CH_2Cl_2, and then 10% conc. NH_4OH in 50% MeOH/CH_2Cl_2 to elute the product. After evaporation of desired fractions, the product **7** was isolated as yellow solid (0.873 g, 93%). The product material was composed of two regioisomers, α- and γ-amide, and used for next step without separation of the isomers. ^{1}H NMR (400 MHz, D_2O): δ 8.66 (s, 1H), 7.56 (d, 1H, *J* = 8.8

Hz), 6.58-6.56 (d, 1H, *J* = 8.8 Hz), 4.50 (s, 2H), 3.25 (m, 2H), 2.68-2.65 (m, 2H), 2.25-2.19 (m, 2H), 2.16-1.8 (m, 2H) ppm. ^{13}C NMR (100 MHz, D_2O): δ 181.53, 178.52, 175.77, 174.63, 172.97, 170.16, 169.26, 163.88, 155.35, 151.13, 150.93, 147.21, 147.09, 129.09, 128.85, 128.04, 121.32, 120.72, 112.47, 112.32, 55.64, 55.04, 54.97, 45.70, 43.61, 41.70, 39.65, 39.50, 33.72, 32.61, 27.72, 27.57 ppm. MS (ESI): *m/z* (relative intensity, %) = 484.19 (100) $[M+H]^+$, 327.11 (51). HRMS (ESI) calcd for $C_{21}H_{26}N_9O_5$ 484.2057, found 484.2067.

2.6 Synthesis of 2 (PAMAM G5-FA9-MTX17)

To a suspension of **6** (PAMAM G5-glutaric acid; 60 mg)[13] in anhydrous DMF (12 mL) was added 4-dimethylaminopyridine (18 mg, 148 μmol), N-hydroxysuccinimide (17 mg, 148 μmol), and 1-ethyl-3-(3-dimethylaminopropyl)carbodiimide hydrochloride (29 mg, 151 μmol). The mixture was stirred at rt for 36 h, and followed by the addition of **7** (18.5 mg, 37.3 μmol) and **5** (TFA salt, freshly prepared from 31 mg of **4**; 37.1 μmol). Then triethylamine (26 μL, 189 μmol) was added to the reaction mixture to adjust the solution to slightly basic (pH~9). The mixture was stirred at rt for 36 h in the dark prior to the addition of water (2 mL). After stirring for 4 h at rt, the mixture was concentrated to a volume of ~2 mL, and diluted with water (15 mL). The solution was added into a into membrane dialysis tubing (MWCO 10 kDa, Spectrum® Labs, Inc.), and dialyzed extensively against deionized water (4 L), phosphate-buffered saline solution (1×2 L), and deionized water (3×4 L) over 3 days. The solution in the tubing was collected and lyophilized, yielding **2** as pale yellow fluffy solid (45 mg). ^{1}H NMR (400 MHz, DMSO-d_6): δ = 8.46 (br), 7.65 (br), 7.48 (br), 7.06 (br), 6.7 (br), 5.35 (br), 4.7 (br), 4.53 (br), 4.38 (br), 3.78 (br s), 3.36 (br s), 3.2-2.8 (br m), 2.7-2.4 (br m), 2.39 (s), 2.38-1.8 (br m), 1.6 (br s) ppm. A set of NMR signals unique to FA/MTX (δ = 8.46, 6.7 ppm) and to *ortho*-nitrobenzyl linker (δ = 7.06, 5.35 ppm) were selected to calculate the relative ratio between **7** and **5** attached per a dendrimer basis: Eq 1 = ratio = [(number of **7**) ÷ (number of **5**) = $N_{FA} \div N_{MTX}$ = 1.84]. Average molecular weight of **2** was obtained by MALDI-TOF with a peak intensity at *m/z* = 57000 $gmol^{-1}$. Increment in the molecular weight of **2** relative to **6** (*m/z* = 40200 $gmol^{-1}$) is attributed to the molecular weight contributed from both **5** and **7** attached to **6**: Eq 2 = Δ wt (unit, $gmol^{-1}$) = (57000 - 40200) = 16800 = [(MW of **7**) × N_{FA} + (MW of **5**) × N_{MTX}] = [483 × N_{FA} + 735× N_{MTX}]. The number of FA and MTX per dendrimer was obtained by solving two equations (Eq 1 and Eq 2), suggesting 9 (**7**) and 17 (**5**), respectively.

2.7 Photolysis of 2

Photolysis experiments were carried out using Spectroline® UV bench lamps (XX-15A; 320–400 nm, power = 1.1 mW/cm^2) at long wavelength (320–400 nm) with a maximum intensity at 360 nm. Nanoconjugate **2** was dissolved in phosphate-buffered saline (PBS) solution (33 μM, pH 7.2), placed in a Petri dish without any cover under UV lamps at distance of ~ 5 cm, and irradiated for a variable period of time up to 14 min. The progress of the photolysis was monitored by analyzing each aliquot taken at a specific time point by UV-vis spectrometry and analytical HPLC. In the HPLC analysis, all samples were eluted using a linear gradient of aqueous acetonitrile (0.1% TFA) at a flow rate of 0.5 mL/min.

2.8 Dihydrofolate reductase (DHFR) assay

Inhibitory activity of dendrimer MTX conjugate **2** against human dihydrofolate reductase (Sigma assay kit) was measured according to the assay protocol as provided. The assay was performed at rt by following the decrease of NADPH and dihydrofolate concentrations by absorbance measurements at 340 nm at different concentrations of the inhibitor as indicted in Figure 5a. The ΔOD (min^{-1}) used for calculating specific enzyme activity (Units/mg P = $\mu molmin^{-1}mg^{-1}$) in each of the inhibition reactions was obtained through the linear fitting of reaction progress in an early phase (0–2.5-min).

2.9 In vitro cell based assay

The *in vitro* cytotoxicity of free MTX, and PAMAM dendrimer nanoconjugates including **2** (intact and following exposure to the UV-A light over a variable period of time) was measured in KB cells using XTT assay. The KB cells, a sub-line of the cervical carcinoma HeLa cells (ATCC, Manassas, VA, USA), were grown as a monolayer cell culture at 37 °C and 5% CO_2 in folic acid-deficient RPMI 1640 medium supplemented with 10% fetal bovine serum (FBS). The 10% FBS provided folic acid concentration equivalent to that present in the human serum (~20 nM). For the cytotoxicity experiments, the cells were seeded in 96-well microtiter plates (3000 cells/well) in serum-containing medium. Two days after plating, the cells were treated with different concentrations of the conjugates in tissue culture medium for 3–4 days. A colorimetric 'XTT' (sodium 3-[1-(phenylaminocarbonyl)-3,4-tetrazolium]-bis (4-methoxy-6-nitro) benzene sulfonicacid hydrate) assay (Roche Molecular Biochemicals, Indianapolis, IN), was performed following the vendor's protocol. After incubation with the XTT labeling mixture, the microtiter plates were read on an ELISA reader (Synergy HT, BioTek) at 492 nm with the reference wavelength at 690 nm.

3. Results and discussion

3.1 Design and synthesis of PAMAM dendrimer conjugated with photocaged methotrexate

We designed a photocaged conjugate **2** (Figure 2) that contains MTX attached through an *ortho*-nitrobenzyl (ONB) group, a linker that can be cleaved by UV irradiation to controllably release MTX molecules from the dendrimer. The structure of conjugate **2** has been modified from the previous conjugate **1** to include a longer spacer (~12 atom), primarily due to the presence of a photocleavable linker itself, and a higher number of FA and MTX molecules, an average of ~9 and ~17, respectively, per dendrimer. We assumed that such modification of the design elements would be potentially beneficial for improving the efficiency of folate receptor-targeted drug delivery due to greater multivalent effect[41–42] (9 FAs), and higher loading capacity of the drug molecules to be delivered (17 MTXs per dendrimer conjugate). This photochemical approach for MTX release was based on the concept of photocaging, which refers to the temporary protection of a biologically active molecule with a photocleavable group. Following UV irradiation, the biologically active molecule, in this case MTX, is released. Photocaging has been employed in a number of chemical and biological applications, including the spatiotemporal control of cell signaling processes[43–45] and the light-triggered release of various payloads from nanomaterials[46–47].

Nanoconjugate **2** was synthesized by covalently coupling the photoreleasable MTX-linker and FA-linker (FA-$CONHCH_2CH_2NH_2$) to the surface of a G5 PAMAM dendrimer (diameter ~5.4 nm[35]). The synthesis of the MTX-photocleavable linker **5** is summarized in Scheme 1. The linker contains an *ortho*-nitrobenzyl (ONB) moiety as a photocleavable group which is attached at the carboxylate oxygen of the L-glutamate domain of MTX. It was synthesized using a two-step process that included the synthesis of **4** from *O*-alkylation of MTX with an ONB-based bifunctional linker **3**[13]. After the *O*-alkylation, **4** was isolated by flash silica column chromatography as a mixture of α- and γ-ester in an approximately equal ratio (on the basis of ^{1}H NMR data; only γ-isomer shown) but their separation was not further pursued because both of the isomers releases MTX upon photocleavage. The *N*-Boc group in **4** was deprotected with TFA to generate a free primary amine at the terminus of the ethylenediamine linker. Second, FA-ethylenediamine **7** (FA-$CONHCH_2CH_2NH_2$) was prepared by amide formation of FA with ethylenediamine as described elsewhere (folic acid dihydrate, 5 eq. of EDC, DMF, rt, 1hr; then 10 eq. of 1,2-diaminoethane, rt, 6 h.)[40].

Synthesis of nanoconjugate **2** was completed as shown in Scheme 2 by covalent conjugation of MTX-linker **5** and FA-linker **7** to PAMAM G5-CO_2H **6** (M_n = 42730 $gmol^{-1}$, PDI = M_w/M_n ~1.046)[13] through amide linkages. In this coupling reaction, the carboxylic acids present on the surface of dendrimer (~100 CO_2H per a dendrimer molecule) were activated to *N*- hydroxysuccinimide esters (EDC/NHS/DMF), and then reacted with **5** and **7** in a one-pot reaction process. The resultant nanoconjugate **2** was purified by extensive dialysis using membrane tubing (MWCO 10 kDa) against phosphate-buffered saline (PBS) solution and water. An analysis that combines spectroscopic and chromatographic data (Figure 3, 4) suggests that **2** has an average molar mass of 57,000 $gmol^{-1}$ (MALDI-TOF MS), and contains ~9 copies of **7** and ~17 copies of **5** by the mean value per dendrimer.

3.2 Photochemical mechanism of methotrexate release

Light-controlled release of MTX from nanoconjugate **2** was carried out by exposing an aqueous solution of the nanoconjugate to 365 nm UV-A light (Figure 2, and 4)[13]. The UV-vis absorption spectra of **2** over time following irradiation are shown in Figure 4a. Prior to irradiation (bottom curve), **2** shows absorption features above 300 nm that reflect a weighted combination of FA (absorption peaks: 280 nm, ε= 25545 $M^{-1}cm^{-1}$; 347 nm, ε = 6676 $M^{-1}cm^{-1}$), MTX (368 nm, ε = 8071 $M^{-1}cm^{-1}$), and the photo-cleavable linker **3** (340 nm, ε = 2750 $M^{-1}cm^{-1}$). Its UV-vis time course shows only minor increases in the absorption peaks at long wavelengths, including 370 nm (inset). However, there is a large increase of absorbance around 284 nm, a spectral feature that was also analogously observed in the photo-cleavage of the ONB linker **3** (quantum efficiency of cleavage, Φ = 0.29)[13]. Reversed phase high performance liquid chromatography (HPLC) analysis of the irradiated solutions of **2** confirmed time-dependent release of MTX, indicating near completion of the release after 6 min of irradiation (Figure 4b). However the HPLC traces also show the appearance of three faster running species at t_r = 0.9 to 1.1 min. We believe that their HPLC and UV/vis profiles are closely related with those of major photodegradation products of MTX which are identified in earlier studies[48–49] as 2,4-diamino-6-pteridinecarbaldehyde, 2,4-diamino-6-pteridinecarboxylic acid, and p-aminobenzoylglutamic acid. In summary, the analysis by UV/vis and HPLC methods demonstrated that UV-A irradiation enabled photochemical

release of MTX from **2** (G5-FA_9-MTX_{17}). However, some fraction of MTX appeared to be degraded into smaller fragments as a function of the exposure time.

3.3 Inhibition of dihydrofolate reductase (DHFR) activity by methotrexate conjugated to PAMAM dendrimer

Biological activity of dendrimer conjugate **2** was investigated with regards to its effect on enzyme activity, and then cell growth. First, we evaluated if **2** is able to inhibit its target enzyme DHFR as its intact form (without MTX release) in a standard enzyme assay using purified human DHFR as described elsewhere38. The results showed that **2** is nearly as potent as free MTX in inhibiting the enzyme activity (Figure 5a), suggesting that MTX tethered to the dendrimer surface is functionally active without being released. This hypothesis is supported by the additional observation that the dendrimer conjugate **2** was quite stable against the hydrolytic release of MTX in aqueous media. Only a small fraction (~2%) of MTX was released after prolonged incubation (48 h) at pH 7.4 which is consistent with the hydrolytic stability associated with the conjugate **1**.

3.4 Effect of drug release on cytotoxicity

Second, nanoconjugate **2** was further evaluated in a cell-based assay[11] using FAR-overexpressing KB cells for its cytotoxicity before and after MTX release controlled by a photochemical mechanism (Figure 5b). Here an aqueous solution of **2** (33 μM per a MTX basis) was dissolved in PBS buffer, pH 7.2 and exposed to UV-A irradiation (365 nm), as described in Figure 3. After exposure for 6 or 14 mins, KB cells were treated with each of the irradiated solutions at different concentrations (based on MTX) for 4 d to evaluate dose-dependent inhibition of cell proliferation (given as % surviving cells). Figure 5b summarizes the dose-cytotoxicity profile of **2** obtained prior to irradiation (t = 0 min, control) and after irradiation (t = 6 or 14 min). The level of cell growth after treatment with **2** (control) was reduced to ~20% relative to normal growth condition (~100%; without any inhibitor or conjugate added), indicating a high level of inhibition activity that was almost identical to that obtained by free MTX. When treated with **2** following 6 and 14 min irradiation, a similar maximal level of inhibitory activity was obtained. However in terms of IC_{50} value[50], **2** (t = 0 or 6 min irradiation) showed ~7 nM, an activity approximately 3-fold less potent than free MTX ($IC_{50} \approx 2.5$ nM). After prolonged irradiation (t = 14 min), a decreased activity ($IC_{50} \approx 15$ nM) was observed. We believe that such decrease in the cytotoxicity is attributable to degradation of MTX molecules to some extent, as suggested by the HPLC traces (Figure 4b). The AUC analysis of each HPLC trace taken after irradiation enabled us to estimate the fraction of intact MTX molecules (excluding the fractions of degraded MTX). This analysis suggests that the real concentrations of MTX remained after irradiation for 6 min and 14 min are ~18 μM, and ≤11 μM, respectively. Thus, the IC_{50} values (7 nM and 15 nM for the 6′ and 14′ incubation samples, respectively, as derived from Fig 5b) are inversely correlated with the amount of MTX as estimated by the AUC analysis.

We have compared the cytotoxicity of the nanoconjugate **2** with a batch of G5-FA_5-$MTX_{7.5}$ standard (pink symbols, Figure 5b). This nanoconjugate, a structural analogue of **1** (Figure 1) that contains different numbers of FA (5) and MTX (7.5) per dendrimer but otherwise an identical structure, has been shown to induce cytotoxicity in KB cells both *in vitro* and *in*

vivo[9, 27]. Here, we show that this conjugate also induces cytotoxicity in KB cells with an IC_{50} value of 150 to 225 nM on a MTX basis. The ~20–30 fold enhancement in potency of conjugate **2** over this standard conjugate G5-FA_5-$MTX_{7.5}$ could be due to i) its increased uptake as a result of the higher average number of targeting molecules per dendrimer (~9 vs. ~5 FAs); ii) its increased toxicity per nanoconjugate as a result of the higher average number of drug molecules per dendrimer (~17 vs. 7.5 MTXs); and/or iii) the addition of the longer tether linking the MTX and G5 at the glutamic acid position to allow perhaps the tighter binding of the MTX-linker construct to the catalytic site of DHFR[19] (Figure 1). Importantly, such longer spacer can reduce the level of undesired steric effects[29, 51–52] which were suggested to explain reduced activity of antibody-targeted MTX-dendrimer conjugates in inhibition of DHFR[29, 51].

4. Conclusions

In conclusion, we demonstrated light-controlled release of MTX using a FAR-targeting, MTX-tethered dendrimer nanoconjugate, and showed that the targeted delivery of active MTX can be achieved, with or without drug release. The photocaging strategy developed here might be able to serve a convenient tool of drug release triggered by a light-controlled mechanism. We believe this strategy can make unique applications in particular when targeting a non-cytosolic therapeutic system localized in a subcellular compartment such as nucleus into which nanoscale particles are unable to passively cross, or if the conjugate carries incorrectly oriented or linked drugs[27]. Our future efforts will focus on such applications through photochemical spatiotemporal drug activation.

Acknowledgments

This work was supported by the National Cancer Institute, National Institutes of Health under award 1 R01 CA119409 (JRB). We thank Dr. Pascale Leroueil for careful review of the manuscript. We appreciate Mr. Suyang Qin for his help in the cell growth assay.

Notes and references

1. Ojima I. Guided Molecular Missiles for Tumor-Targeting Chemotherapy; Case Studies Using the Second-Generation Taxoids as Warheads. Acc Chem Res. 2008; 41:108–119. [PubMed: 17663526]
2. Ghosh SK, Pal A, Kundu S, Nath S, Pal T. Fluorescence quenching of 1-methylaminopyrene near gold nanoparticles: size regime dependence of the small metallic particles. Chemical Physics Letters. 2004; 395:366–372.
3. Feazell RP, Nakayama-Ratchford N, Dai H, Lippard SJ. Soluble Single-Walled Carbon Nanotubes as Longboat Delivery Systems for Platinum(IV) Anticancer Drug Design. J Am Chem Soc. 2007; 129:8438–8439. [PubMed: 17569542]
4. Dubowchik GM, Walker MA. Receptor-mediated and enzyme-dependent targeting of cytotoxic anticancer drugs. Pharmacol Therap. 1999; 83:67–123. [PubMed: 10511457]
5. Majoros IJ, Williams CR, Becker A, Baker JR Jr. Methotrexate delivery via folate targeted dendrimer-based nanotherapeutic platform. WIREs: Nanomed Nanobiotech. 2009; 1:502–510.
6. Low PS, Kularatne SA. Folate-targeted therapeutic and imaging agents for cancer. Curr Opin Chem Biol. 2009; 13:1–7. [PubMed: 19272831]
7. Dvir T, Banghart MR, Timko BP, Langer R, Kohane DS. Photo-Targeted Nanoparticles. Nano Letters. 2009; 10:250–254. [PubMed: 19904979]

8. Majoros IJ, Myc A, Thomas T, Mehta CB, Baker JR. PAMAM Dendrimer-Based Multifunctional Conjugate for Cancer Therapy: Synthesis, Characterization, and Functionality. Biomacromol. 2006; 7:572–579.
9. Thomas TP, Majoros IJ, Kotlyar A, Kukowska-Latallo JF, Bielinska A, Myc A, Baker JR Jr. Targeting and Inhibition of Cell Growth by an Engineered Dendritic Nanodevice. J Med Chem. 2005; 48:3729–3735. [PubMed: 15916424]
10. Thomas TP, Choi SK, Li M-H, Kotlyar A, Baker JR Jr. Design of Riboflavin-presenting PAMAM Dendrimers as a New Nanoplatform for Cancer-targeted Delivery. Bioorg Med Chem Lett. 2010; 20:5191–5194. [PubMed: 20659800]
11. Majoros IJ, Thomas TP, Mehta CB, Baker JR Jr. Poly(amidoamine) Dendrimer-Based Multifunctional Engineered Nanodevice for Cancer Therapy. J Med Chem. 2005; 48:5892–5899. [PubMed: 16161993]
12. Etrych T, Mrkvan T, Říhová, Ulbrich K. Star-shaped immunoglobulin-containing HPMA-based conjugates with doxorubicin for cancer therapy. J Controlled Release. 2007; 122:31–38.
13. Choi SK, Thomas T, Li M, Kotlyar A, Desai A, Baker JR Jr. Light-controlled release of caged doxorubicin from folate receptor-targeting PAMAM dendrimer nanoconjugate. Chem Commun. 2010; 46:2632–2634.
14. Bareford LM, Swaan PW. Endocytic mechanisms for targeted drug delivery. Adv Drug Deliv Rev. 2007; 59:748–758. [PubMed: 17659804]
15. Majoros, I.; Baker, J, Jr. Dendrimer-Based Nanomedicine. Pan Stanford; Hackensack, NJ: 2008. p. 436
16. Joshi A, Vance D, Rai P, Thiyagarajan A, Kane RS. The Design of Polyvalent Therapeutics. Chem Eur J. 2008; 14:7738–7747. [PubMed: 18553325]
17. Plantinga A, Witte A, Li M-H, Harmon A, Choi SK, Banaszak Holl MM, Orr BG, Baker JR Jr, Sinniah K. Bioanalytical Screening of Riboflavin Antagonists for Targeted Drug Delivery—A Thermodynamic and Kinetic Study. ACS Med Chem Lett. 2011; 2:363–367. [PubMed: 21686082]
18. Schnell JR, Dyson HJ, Wright PE. Strcuture, dynamics, and catalytic function of dihydrofolate. Annu Rev Biophys Biomol Struct. 2004; 33:119–140. [PubMed: 15139807]
19. Mauldin RV, Carroll MJ, Lee AL. Dynamic Dysfunction in Dihydrofolate Reductase Results from Antifolate Drug Binding: Modulation of Dynamics within a Structural State. Structure. 2009; 17:386–394. [PubMed: 19278653]
20. Williams JW, Morrison JF, Duggleby RG. Methotrexate, a high- affinity pseudosubstrate of dihydrofolate reductase. Biochem. 2002; 18:2567–2573. [PubMed: 36135]
21. Chunduru S, Cody V, Luft J, Pangborn W, Appleman J, Blakley R. Methotrexate-resistant variants of human dihydrofolate reductase. Effects of Phe31 substitutions. J Biol Chem. 1994; 269:9547–9555. [PubMed: 8144541]
22. Cody V, Luft JR, Pangborn W. Understanding the role of Leu22 variants in methotrexate resistance: comparison of wild-type and Leu22Arg variant mouse and human dihydrofolate reductase ternary crystal complexes with methotrexate and NADPH. Acta Crystallogr D Biol Crystallogr. 2005; 61(Pt 2):147–155. [PubMed: 15681865]
23. Tattersall MHN, Brown B, Frei E. The reversal of methotrexate toxicity by thymidine with maintenance of antitumour effects. Nature. 1975; 253:198–200. [PubMed: 1078601]
24. Kosloski MJ, Rosen F, Milholland RJ, Papahadjopoulos D. Effect of Lipid Vesicle (Liposome) Encapsulation of Methotrexate on Its Chemotherapeutic Efficacy in Solid Rodent Tumors. Cancer Res. 1978; 38:2848–2853. [PubMed: 581069]
25. Chatelut E, Suh P, Kim S. Sustained-release methotrexate for intracavitary chemotherapy. J Pharma Sci. 1994; 83:429–432.
26. Myc A, Majoros IJ, Thomas TP, Baker JR Jr. Dendrimer-Based Targeted Delivery of an Apoptotic Sensor in Cancer Cells. Biomacromol. 2007; 8:13–18.
27. Kukowska-Latallo JF, Candido KA, Cao Z, Nigavekar SS, Majoros IJ, Thomas TP, Balogh LP, Khan MK, Baker JR Jr. Nanoparticle Targeting of Anticancer Drug Improves Therapeutic Response in Animal Model of Human Epithelial Cancer. Cancer Res. 2005; 65:5317–5324. [PubMed: 15958579]

28. Kaminskas LM, Kelly BD, McLeod VM, Boyd BJ, Krippner GY, Williams ED, Porter CJH. Pharmacokinetics and Tumor Disposition of PEGylated, Methotrexate Conjugated Poly-l-lysine Dendrimers. Mol Pharma. 2009; 6:1190–1204.
29. Wu G, Barth RF, Yang W, Kawabata S, Zhang L, Green-Church K. Targeted delivery of methotrexate to epidermal growth factor receptor-positive brain tumors by means of cetuximab (IMC-C225) dendrimer bioconjugates. Mol Cancer Ther. 2006; 5:52–59. [PubMed: 16432162]
30. Chau Y, Dang NM, Tan FE, Langer R. Investigation of targeting mechanism of new dextran-peptide-methotrexate conjugates using biodistribution study in matrix-metalloproteinase-overexpressing tumor xenograft model. J Pharma Sci. 2006; 95:542–551.
31. Bai KB, Lng O, Orbn E, Szab R, Köhidai L, Hudecz F, Mez G. Design, Synthesis, and In Vitro Activity of Novel Drug Delivery Systems Containing Tuftsin Derivatives and Methotrexate. Bioconj Chem. 2008; 19:2260–2269.
32. Han J, Lim S-J, Lee M-K, Kim C-K. Altered Pharmacokinetics and Liver Targetability of Methotrexate by Conjugation with Lactosylated Albumins. Drug Delivery. 2001; 8:125–134. [PubMed: 11570592]
33. Kohler N, Sun C, Wang J, Zhang M. Methotrexate-Modified Superparamagnetic Nanoparticles and Their Intracellular Uptake into Human Cancer Cells. Langmuir. 2005; 21:8858–8864. [PubMed: 16142971]
34. Kamen BA, Capdevila A. Receptor-mediated folate accumulation is regulated by the cellular folate content. Proc Natl Acad Sci USA. 1986; 83:5983–5987. [PubMed: 3461471]
35. Tomalia DA, Naylor AM, William A, Goddard I. Starburst Dendrimers: Molecular-Level Control of Size, Shape, Surface Chemistry, Topology, and Flexibility from Atoms to Macroscopic Matter. Angew Chem Int Ed. 1990; 29:138–175.
36. Lee RJ, Wang S, Low PS. Measurement of endosome pH following folate receptor-mediated endocytosis. Biochim Biophys Acta (BBA) - Mol Cell Res. 1996:237–242.
37. Yang J, Chen H, Vlahov IR, Cheng J-X, Low PS. Characterization of the pH of Folate Receptor-Containing Endosomes and the Rate of Hydrolysis of Internalized Acid-Labile Folate-Drug Conjugates. J Pharmacol Exp Ther. 2007; 321:462–468. [PubMed: 17289839]
38. Thomas, TP.; Kukowska-Latallo, JR. Biological application of PAMAM dendrimer nanodevices in vitro and in vivo. In: Majoros, I.; Baker, JR., Jr, editors. Dendrimer-Based Nanomedicine. Pan Stanford; Hackensack, NJ: 2008. p. 175-207.
39. Li M-H, Choi SK, Thomas TP, Desai A, Lee K-H, Kotlyar A, Banaszak Holl MM, Baker JR Jr. Dendrimer-based Multivalent Methotrexates as Dual Acting Nanoconjugates for Cancer Cell Targeting. Eur J Med Chem. 2012; 4710.1016/j.ejmech.2011.1011.1027
40. Whiteley JM, Henderson GB, Russell A, Singh P, Zevely EM. The isolation of dihydrofolate reductases by affinity chromatography on folate-Sepharose. Anal Biochem. 1977; 79:42–51. [PubMed: 405885]
41. Mammen M, Choi SK, Whitesides GM. Polyvalent interactions in biological systems: implications for design and use of multivalent ligands and inhibitors. Angew Chem Int Ed. 1998; 37:2754–2794.
42. Hong S, Leroueil PR, Majoros IJ, Orr BG, Baker JR Jr, Banaszak Holl MM. The Binding Avidity of a Nanoparticle-Based Multivalent Targeted Drug Delivery Platform. Chem Biol. 2007; 14:107–115. [PubMed: 17254956]
43. Lemke EA, Summerer D, Geierstanger BH, Brittain SM, Schultz PG. Control of protein phosphorylation with a genetically encoded photocaged amino acid. Nature Chem Biol. 2007; 3:769–772. [PubMed: 17965709]
44. Goard M, Aakalu G, Fedoryak OD, Quinonez C, St Julien J, Poteet SJ, Schuman EM, Dore TM. Light-Mediated Inhibition of Protein Synthesis. Chem Biol. 2005; 12:685–693. [PubMed: 15975514]
45. Furuta T, Wang SSH, Dantzker JL, Dore TM, Bybee WJ, Callaway EM, Denk W, Tsien RY. Brominated 7-hydroxycoumarin-4-ylmethyls: Photolabile protecting groups with biologically useful cross-sections for two photon photolysis. Proc Natl Acad Sci USA. 1999; 96:1193–1200. [PubMed: 9990000]

46. Mal NK, Fujiwara M, Tanaka Y. Photocontrolled reversible release of guest molecules from coumarin-modified mesoporous silica. Nature. 2003; 421:350–353. [PubMed: 12540896]

47. Agasti SS, Chompoosor A, You C-C, Ghosh P, Kim CK, Rotello VM. Photoregulated Release of Caged Anticancer Drugs from Gold Nanoparticles. J Am Chem Soc. 2009; 131:5728–5729. [PubMed: 19351115]

48. Chatterji DC, Gallelli JF. Thermal and photolytic decomposition of methotrexate in aqueous solutions. J Pharm Sci. 1978; 67:526–531. [PubMed: 641762]

49. Chahidi C, Giraud M, Aubailly M, Valla A, Santus R. 2,4- Diamino-6-pteridinecarboxaldehyde and an azobenzene derivative are produced by UV photodegradation of methotrexate. Photochem Photobiol. 1986; 44:231–233. [PubMed: 3774890]

50. IC_{50} is defined as the concentration of **2** (per an MTX basis) that inhibited the cell growth at the level halfway between control (100%) and maximal inhibition (~20%).

51. Shukla R, Thomas TP, Desai AM, Kotlyar A, Park SJ, Baker JR Jr. HER2 specific delivery of methotrexate by dendrimer conjugated anti-HER2 mAb. Nanotechnology. 2008; 19:295102. [PubMed: 20686639]

52. Choi SK, Leroueil P, Li M-H, Desai A, Zong H, Van Der Spek AFL, Baker JR Jr. Specificity and Negative Cooperativity in Dendrimer–Oxime Drug Complexation. Macromol. 2011; 44:4026–4029.

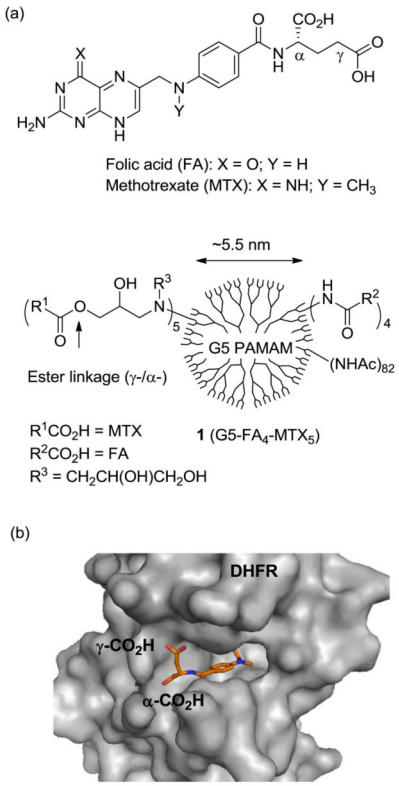

Fig. 1.

(a) Structures of folic acid (FA), methotrexate (MTX), and a multifunctional nanoconjugate **1** based on a fifth generation (G5) polyamidoamine (PAMAM) dendrimer where folic acid as a targeting ligand and methotrexate as a chemotherapeutic agent are conjugated to surface residues; (b) A crystal structure of human dihydrofolate reductase (hDHFR) at the active site with a bound MTX molecule, each shown in a surface (protein) and stick (MTX) representation where the L-glutamate carboxylic acids (α, γ) of MTX appear to be anchored near the entrance leading to a catalytic pocket, while its pteridine head group (hidden) is bound deep into the pocket (PDB 1u72)[22].

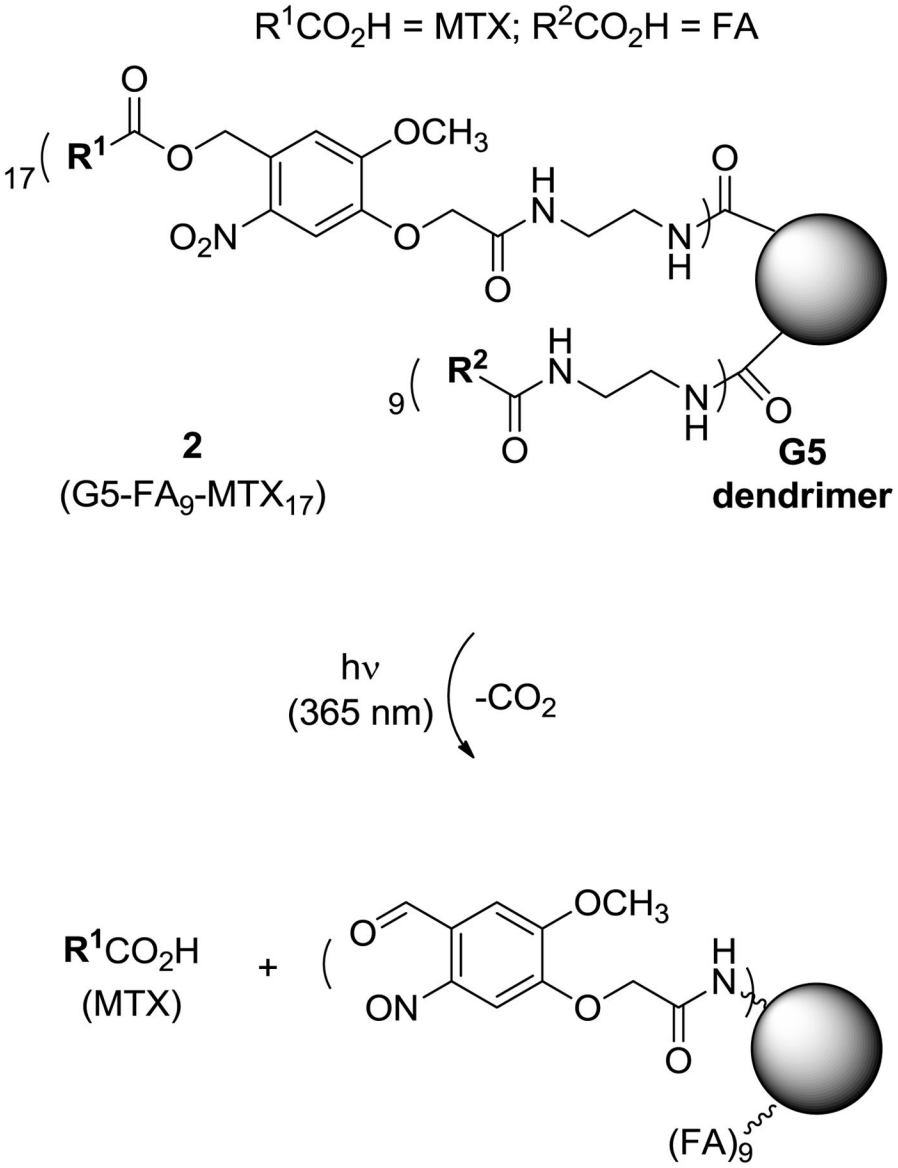

Fig. 2.

Photocontrolled release of methotrexate (MTX) from a nanoconjugate **2** (G5-FA_9-MTX_{17}) upon exposure to UV irradiation (365 nm) as the result of the cleavage of *ortho*-nitrobenzyl (ONB) linker.

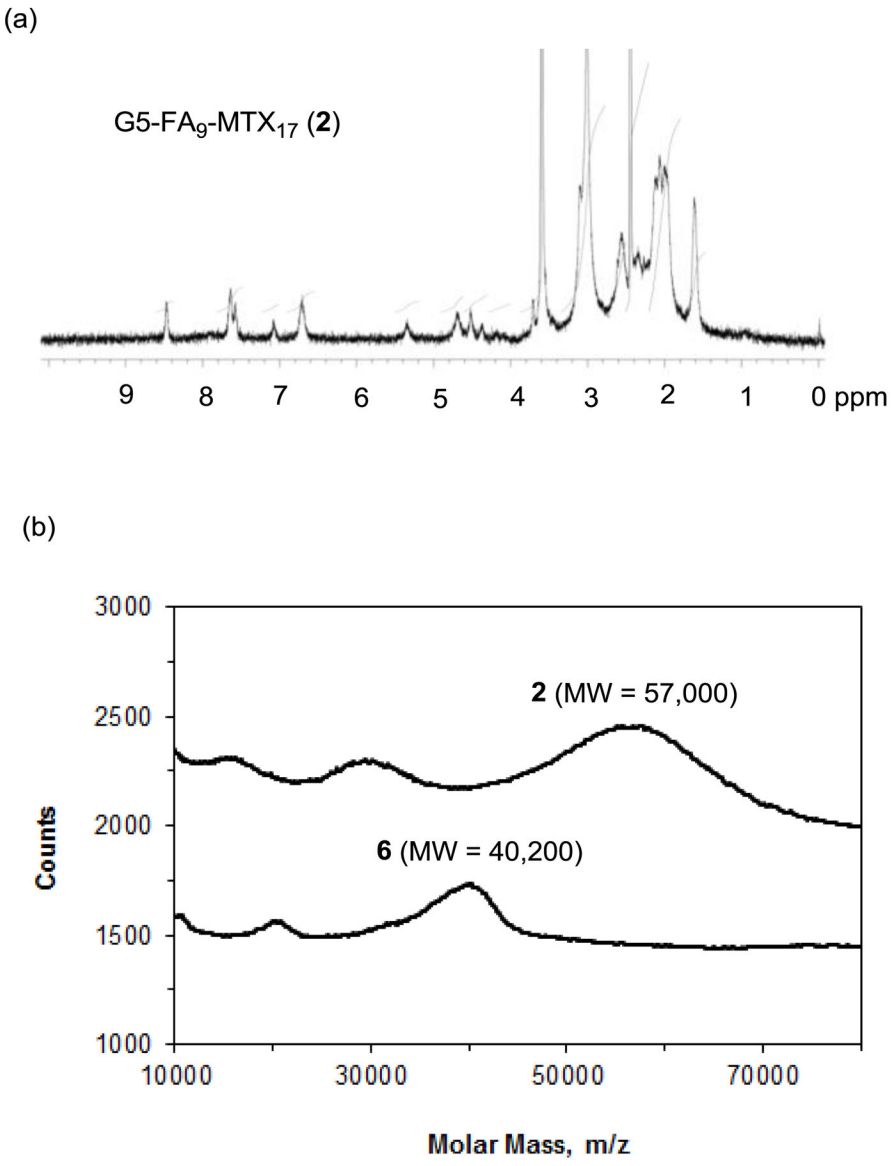

Fig. 3.

(a) ^{1}H NMR spectrum of **2** (G5-FA_9-MTX_{17}) obtained in a mixture of DMSO-d_6 and D_2O; (b) MALDI TOF mass spectral data ($gmol^{-1}$) for the dendrimer conjugate **2**, and **6**.

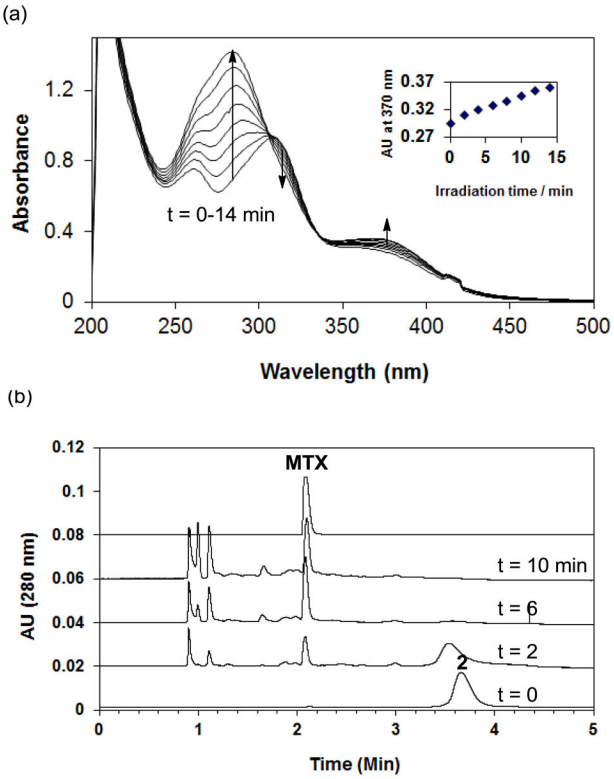

Fig. 4.

Photocontrolled release of MTX from **2** (G5-FA_9-MTX_{17}) upon exposure to UV-A (365 nm) irradiation. An aqueous solution of **2** (33 μM in PBS, pH 7.4) was exposed to the long wave length irradiation over a variable period of time (t = 0 to 14 min). During the course of photolysis of **2**, release of MTX was monitored by UV-vis spectroscopy (a), and analytical high performance liquid chromatography (b) in which a select set of HPLC traces taken before (t = 0 min) and after UV irradiation (t = 2 to 10 min) are shown. Absorption (HPLC) at 280 nm is shown to focus on MTX rather than G5 dendrimer backbone.

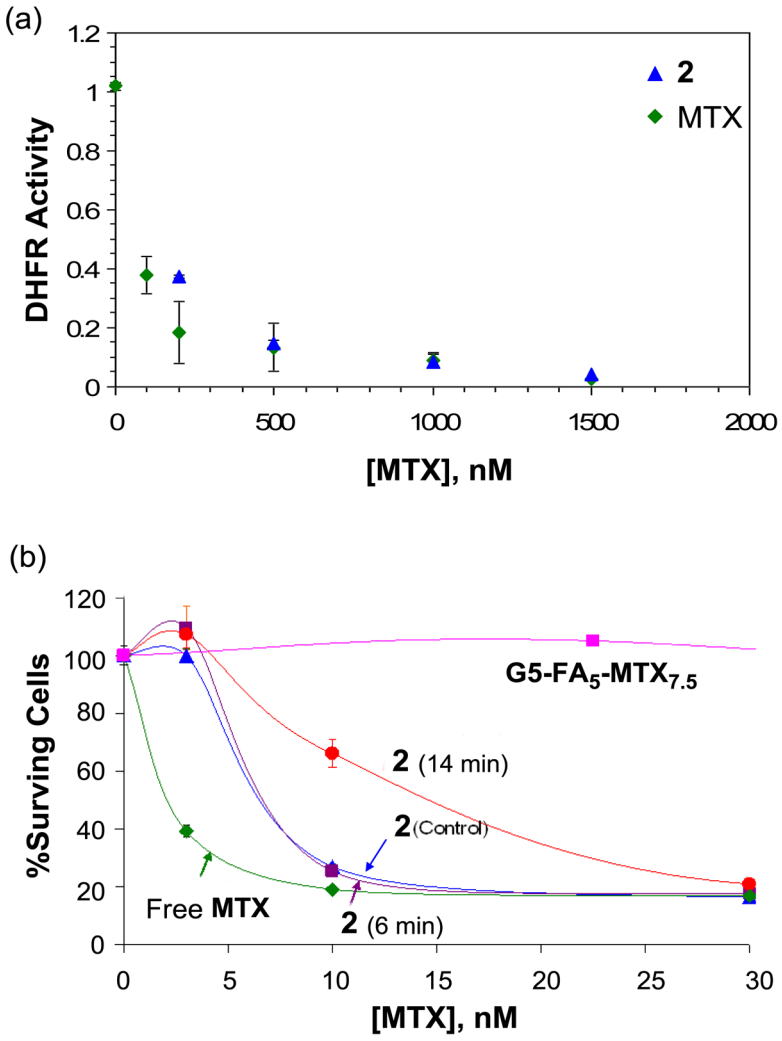

Fig. 5.

(a) Inhibition of human dihydrofolate reductase (hDHFR) by **2** (G5-FA_9-MTX_{17}) in a cell-free enzyme assay. The unit for DHFR activity is defined as μmolmin^{-1}mg^{-1}, and the concentrations for **2** on the X-axis are given on a MTX basis; (b) *In vitro* cytotoxicity of **2** in a cell-based assay using folate receptor-overexpressing KB cells, before (control) and after UV-irradiation (6, or 14 mins). The standard comparator, G5-FA_5-$MTX_{7.5}$ (see text) showed ~20% cell growth inhibition at 75 nM (equivalent to 10 nM on a conjugate basis; data point not shown on the graph). The concentrations shown on the X-axis are given on a MTX basis.

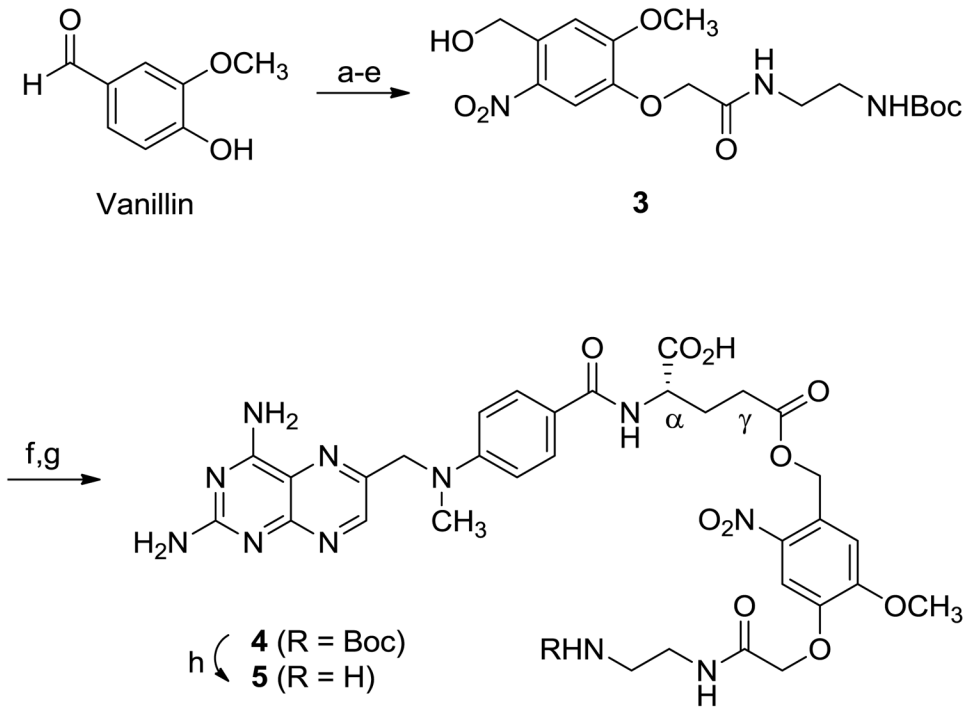

Scheme 1.

Synthesis of MTX-photocleavable linker **5**. *Reagents and conditions*: a) ethyl bromoacetate, K_2CO_3, DMF, rt, 17 h, 75%; b) NaOH, THF, MeOH, H_2O, rt, 33 h, 82%; c) conc. HNO_3, AcOH, 0°C to rt, 26 h, 68%; d) *N*-Boc-1,2-diaminoethane, DCC, DMAP, DMF, 0°C to rt, 36 h, 88%; e) $NaBH_4$, THF, MeOH, rt, 5 h, 71%; f) methanesulfonyl chloride, Et_3N, $CHCl_3$, 0°C→rt, 2 h; g) Cs_2CO_3, NaI, methotrexate, DMF, rt, 27 h, 23% over two steps; h) TFA, $CHCl_3$, rt, 15 min. DMF = dimethylformamide, THF = tetrahydrofuran, DCC = dicyclohexylcarbodiimide, DMAP = 4-dimethylaminopyridine, Et_3N = triethylamine, TFA = trifluoroacetic acid.

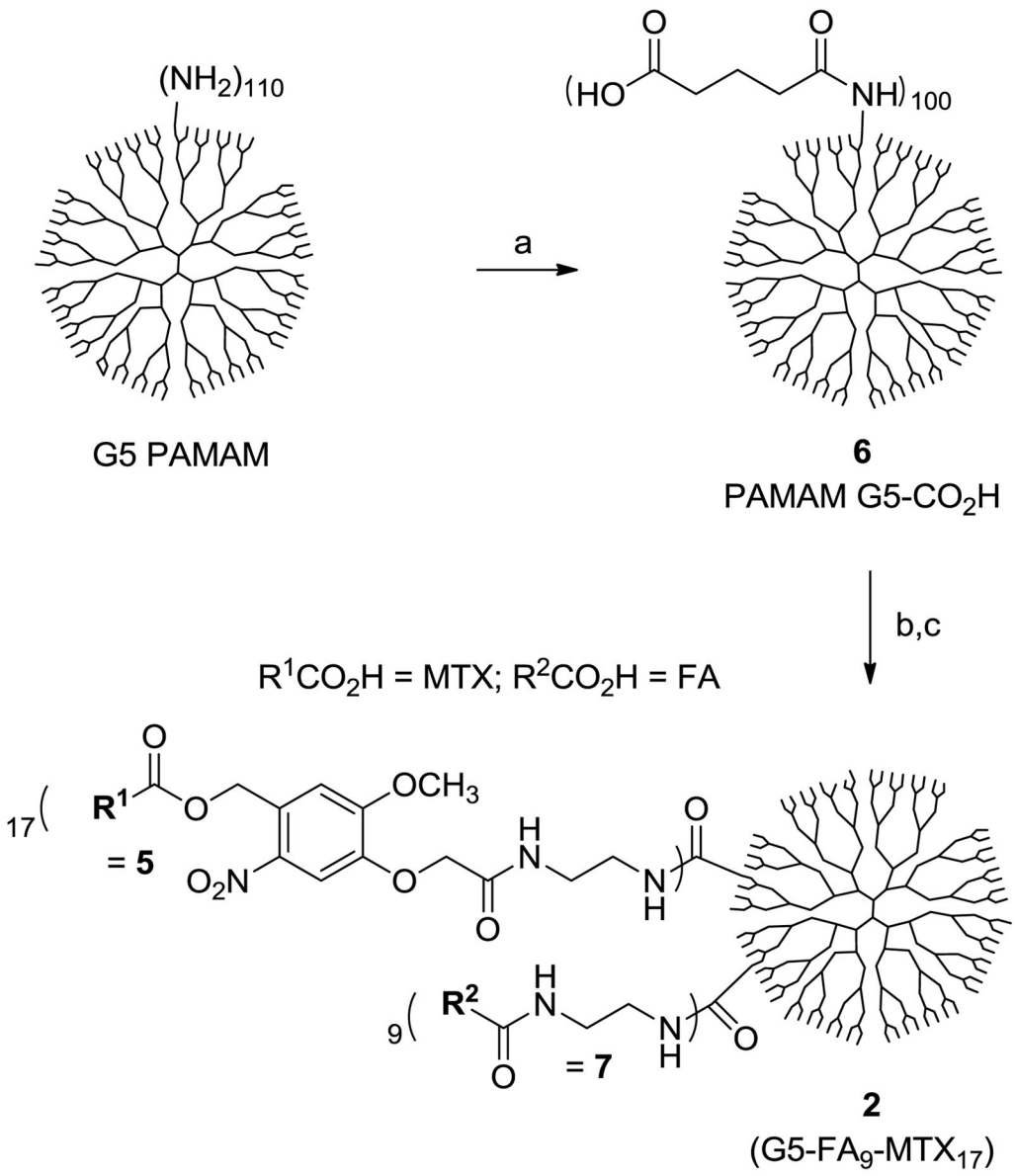

Scheme 2.

Synthesis of a fifth generation (G5) PAMAM dendrimer-based nanoconjugate **2** (G5-FA_9-MTX_{17}). *Reagents and conditions*: a) glutaric anhydride, Et_3N, MeOH, rt, 24 h; b) NHS, EDC, DMAP, DMF, rt, 36 h; c) **5** (methotrexate-photocleavable linker, 25 mol. eq per a dendrimer basis), **7** (FA-$CONHCH_2CH_2NH_2$, 25 mol. eq per a dendrimer basis), Et_3N, DMF, rt, 36 h; then dialysis (MWCO10 kDa) against phosphate-buffered saline (PBS) and H_2O. NHS = *N*-hydroxysuccinimide, EDC = 1-ethyl-3-(3-dimethylaminopropyl)carbodiimide hydrochloride.